Biomedical Physics & Engineering Express

ENDORSED BY IPEM Institute of Physics and Engineering in Medicine

ACCEPTED MANUSCRIPT • OPEN ACCESS

Electrospun gelatin-based scaffolds as a novel 3D platform to study the function of contractile smooth muscle cells *in vitro*

To cite this article before publication: Jack C Bridge *et al* 2018 *Biomed. Phys. Eng. Express* in press https://doi.org/10.1088/2057-1976/aace8f

Electrospun gelatin-based scaffolds as a novel 3D platform to study the function of contractile smooth muscle cells *in vitro*

Bridge J.C.[1,2*], M. Amer[1*], G.E. Morris[1], N.R.W. Martin[2], D.J. Player[2,5], A.J. Knox[3], J.W. Aylott[1], M.P. Lewis[2,3], F.R.A.J. Rose[1$]

1. Division of Regenerative Medicine and Cellular Therapies, Centre for Biomolecular Sciences, School of Pharmacy, University of Nottingham, UK. 2. School of Sport, Exercise and Health Sciences, Loughborough University, UK. 3. National Centre for Sport and Exercise Medicine, Loughborough University, UK. 4. Division of Respiratory Medicine, School of Clinical Sciences, University of Nottingham, UK. 5. Institute of Orthopaedics and Musculoskeletal Science, Division of Surgery and Interventional Science, University College London, UK

[*]Joint first author

[$]Corresponding author

Corresponding author:

Felicity RAJ Rose
Division of Regenerative Medicine and Cellular Therapies
School of Pharmacy
Centre for Biomolecular Sciences
University of Nottingham
Nottingham, UK
felicity.rose@nottingham.ac.uk

Running Title

Electrospun scaffolds for the assessment of function of contractile smooth muscle cells

Abstract

Contractile dysfunction of smooth muscle (SM) is a feature of chronic cardiovascular, respiratory and gastro-intestinal diseases. Owing to the low availability of human *ex vivo* tissue for the assessment of SM contractile function, the aim of this study was to develop a novel *in vitro* SM model that possesses the ability to contract, and a method to measure its contractility. A range of electrospun scaffolds were produced from crosslinked gelatin and methacrylated gelatin (GelMA), generating highly aligned scaffolds with average fibre diameters ranging from 200 nm to several micrometres. Young's moduli of the scaffolds ranged from $1x10^5$ to $1x10^7$ Pa. Primary aortic smooth muscle cells (AoSMCs; rat) cells readily adhered to and proliferated on the fibrous scaffolds for up to 10 days. They formed highly aligned populations following the topographical cues of the aligned scaffolds and stained positive for SM markers, indicating a contractile phenotype. Cell-seeded GelMA scaffolds were able, upon stimulation with uridine 5'-triphosphate (UTP), to contract and their attachment to a force transducer allowed the force of contraction to be measured. Hence, these electrospun GelMA fibres can be used as biomimetic scaffolds for SM cell culture and *in vitro* model development, and enables the contractile forces generated by the aligned three-dimensional sheet of cells to be directly measured. This will supplement *in vitro* drug screening tools and facilitate discovery of disease mechanisms.

Keywords: Electrospinning, 3D Cell Culture, Contractile, Smooth Muscle, Tissue Engineering, *In vitro* model, GelMA.

1. Introduction

Smooth muscle (SM) is a key component of respiratory, cardiovascular, and gastrointestinal systems. Certain disease states arise due to dysfunction in the smooth muscle component and, as yet, such diseases not fully understood; an example is asthma [1]. Technical and ethical difficulties associated with *in vivo* human research and the maintenance of human primary cells *in vitro* have significantly limited studies aimed at elucidating the interrelationship between the main cell types and the extracellular matrix involved in such pathologies. In addition, the low availability of human tissue suitable for *ex vivo* assessment of contractile function has restricted current methods for studying smooth muscle (such as airway smooth muscle; ASM) to those that require *ex vivo* tissues, animal models or 2D *in vitro* systems [2]. Conventional 2D culture models represent a non-physiological mechanical environment where contraction is assessed at a single cell level. *Ex vivo* models replicate the *in vivo* situation *in vitro* but these techniques (such as the precision cut lung slice model) are technically challenging, the cell and matrix components cannot be easily manipulated, and the construct is essentially dying during the experiment. Currently available animal models represent poor relevance to human disease and only mimic aspects of the human phenotype [3].

Tissue engineering principles have been applied to the generation of 3D culture models created using cells *in vitro* cultured on a 3D scaffold to provide a more physiologically relevant environment than 2D cultures [4]. Natural polymers, such as collagen [5] and gelatin, exhibit high cellular biocompatibility and are more elastic in nature than synthetic polymers (e.g.: poly(ethylene terephthalate) PET) [6]. Electrospinning produces fibrous, porous, 3D scaffolds that resemble the structure of the natural extracellular matrix [7]. Fluorinated alcohols used as electrospinning solvents have been reported to cause denaturation of collagen [8, 9]. As a result, there is little difference between the resultant electrospun collagen fibres when compared to those fabricated from gelatin [10]. Therefore, as an alternative to collagen, electrospinning gelatin is a more cost-effective way of producing scaffolds that are chemically similar to collagen whilst still being biocompatible and biodegradable [11].

Crosslinking gelatin provides stability against enzymatic degradation, lower water solubility and an opportunity to modulate mechanical properties [12]. Gelatin methacrylate (GelMA), synthesised via a reaction between gelatin and methacrylic anhydride, consists of multiple methacrylamide groups [13]. These can form chemical crosslinks between gelatin molecules in the presence of free radicals from a photoinitiator following light exposure allowing the

tuning of the mechanical and degradation properties of the resultant scaffold. GelMA has been utilised in hydrogel cultures [14-16], micro-patterning [17], and 3D-printing [18, 19]. Three dimensional (3D) GelMA hydrogels closely resemble the native extracellular matrix (ECM) due to the presence of cell-attachment and matrix metalloproteinase responsive peptide motifs [20, 21]. GelMA has been used to coat electrospun polycaprolactone fibres [22] and has recently been electrospun into nanofibre scaffolds to investigate wound healing and cutaneous regeneration [23, 24].

Despite the clear clinical need for more effective therapeutics to treat disease, such as asthma, that involve the SM component, very few new classes of drugs have made it to the clinic over the past 40 years and it is clear that one of the reasons for this is the lack of relevant *in vitro* and *in vivo* models [26]. A tissue engineered approach allows the generation of 'living' tissue constructs from both animal (validation), and human cells (relevance) which can be used to accurately measure contraction. One approach to study SMC function is to decellularise native vessels and/or cross-link them for arterial grafting [27, 28]. Although this does provide a native ECM with some preservation of structure and biochemical composition, the acquisition of native vessels for decellularisation is limited and suffers from issues with sample-to-sample variability. In addition, this approach is extremely limited in the study of paediatric disease (due to the lack of tissue donated for research purposes). These aspects limit the application of this approach.

We have previously reported that electrospun PET scaffolds allow control over fibre alignment, allowing the generation of aligned sheets of smooth muscle [7]. Given that the Young's moduli of *in vivo* SM, such as human arteries, range from 0.1 to 1.0 MPa [25], which is 100-1000 times lower than values reported for the Young's moduli of synthetic fibrous scaffolds (for example those electrospun from PET exhibiting a Young's modulus of 200-300 MPa [7]), we set out to develop a GelMA-based model that provides a suitable matrix for culture of SMCs. This presents a standardised culture platform that bypasses the need for native tissue and allows tailoring of the scaffold's mechanical properties. The aim and novelty of this study therefore was to develop an *in vitro* model of SM that possesses the ability to contract and importantly, to develop a method to directly and quantitatively measure this contractility.

2. Materials and methods

2.1 Synthesis of gelatin methacrylate

Gelatin methacrylate (GelMA) was synthesised following a previously published method [14]. Briefly, 10g of gelatin (type A 300 bloom) was dissolved in 95 mL PBS at 50°C and stirred for 1 hour. Methacrylic anhydride (8.0 mL) was added to the gelatin solution and stirred for a further 3 hours at 50°C. PBS (400 mL) was added to the mixture and stirred for an additional 30 minutes. The solution was then transferred into three dialysis membranes (12-14 kDa molecular weight cut-off). The membranes were placed in 3.0 L of distilled water and stirred at 50°C. The dialysis water was changed twice daily for 7 days before the membranes were removed and the solution frozen overnight at -80°C. The frozen GelMA solution was lyophilised and stored at room temperature. The percentage of methacrylation within the synthesised GelMA was calculated using the following equation:

$$DM\%=I5.6ppm\times0.3836I0.84ppm\times0.0385\times100$$

2.2 Production of electrospun gelatin and GelMA scaffolds

Solutions of gelatin at various concentrations (6, 8 and 10% w/v) were made by dissolving gelatin powder (type A 300 bloom) (Sigma Aldrich, Dorset, UK) in 100% hexafluoroisopropanol (HFIP) (Sigma Aldrich). Solutions of GelMA at 10% *w/v* were made by dissolving freeze-dried GelMA directly into hexafluoroisopropanol (HFIP) (Sigma Aldrich). Solutions were stirred using a magnetic stirrer overnight at 37°C. The gelatin solutions were added to a 5mL syringe with an 18G blunt tip needle attached (BD Falcon™, Oxford, UK) and electrospun at ambient temperature and humidity in a ventilated fume cabinet. For each scaffold, 4 mL of solution was electrospun at a flow rate of 1.2 mL h^{-1}. The needle collector distance was 15 cm and the voltage across the apparatus was 15 kV. The collector mandrel was set to spin at a speed of 2000 rpm. Upon completion of electrospinning, scaffolds were cut from the mandrel using a scalpel blade and stored in aluminium foil at room temperature.

2.3 Crosslinking of electrospun gelatin scaffolds

Prior to crosslinking the scaffolds, they were first secured in an acetate frame (5star™, Cambridge, UK) using aquarium sealant (Sinclair animal and household care Ltd., Gainsborough, UK) on either side of the scaffold. The acetate frame size was either 23 x 42 mm with an internal window of 13 x 32 mm or 25 x 25 mm with an internal window of 15 x 15 mm. Once the acetate frames were adhered, individual scaffolds were cut out and left to dry overnight (**Figure S1**). The gelatin scaffolds were crosslinked with EDC and NHS [29], whereby a solution of 250 mM 1-Ethyl-3-(3-dimethylaminopropyl) carbodiimide (EDC) (Applichem, Darmstadt, Germany) and 100 mM N-Hydroxysuccinimide (NHS) (TCI Europe, Zwijndrecht, Belgium) was prepared in distilled water. Ethanol (Sigma Aldrich) was added to the solution until the total volume was 10 times the original volume. Scaffolds were then placed in the EDC/NHS solution for 24 hours at 4°C and washed in distilled water (x3) before being lyophilised overnight.

2.4 Crosslinking of GelMA scaffolds

Prior to crosslinking, GelMA scaffolds were first secured to an acetate frame (Section 2.3). Scaffolds were then submerged in a 1% *w/v* solution of 2-Hydroxy-4′-(2-hydroxyethoxy)-2-methylpropiophenone (photoinitiator) in a solvent mix of ethanol and water. Solvent ratios used ranged from 1:0 to 9:1 ethanol:water. Scaffolds were then exposed to UV radiation (0.5 Wm^2) for 10 minutes and washed in PBS three times. The proposed mechanism of the crosslinking process is displayed in **Figure S2**; no further crosslinking of the sample occurs when UV sterilised for cell culture due to the wash step removing excess photoinitiator. Samples used for SEM imaging were washed in dH_2O and freeze-dried prior to analysis. Samples used for cell culture were incubated in antibiotic/antimycotic solution (50000 $unitsmL^{-1}$ penicillin G, 500 $mgmL^{-1}$ streptomycin sulphate and 125 μgmL^{-1} amphotericin B) (Fisher Scientific) in PBS at 4°C prior to use.

2.5 NMR analysis

Samples of gelatin and GelMA (as synthesised) were dissolved in D_2O in glass NMR tubes and the NMR spectrum of each sample was determined using a Bruker Avance 600MHz spectrometer (Bruker, Coventry, UK). Spectra were analysed using the MestReNova LITE software package (Mestrelab research, Hereford, UK).

2.6 Scaffold Morphology

Samples of electrospun scaffolds were cut using an 8.0 mm diameter biopsy pen and mounted on a holder using graphite adhesive SEM pads (Agar Scientific, Essex, UK). Samples were gold coated for 5 minutes (Balzers Union SCD 030, Balzers Union Ltd., Liechtenstein) and were then imaged at 20-30 kV using a scanning electron microscope (JEOL JMS-6060 LV, JEOL Ltd., Hertfordshire, UK) at different magnifications (as identified on the images). Scaffold fibre diameter and fibre alignment were determined by analysis of SEM micrographs using the image analysis software packages MeasureIT (Olympus Soft Imaging solutions GmbH, Münster, Germany) and ImageJ respectively. Alignment was calculated by expressing individual fibre angles as deviations from the sample mean fibre angle. All measurements were achieved by measuring 20 fibres from images of 3 individual scaffolds (60 fibres in total).

2.7 Tensile measurements of GelMA scaffolds

Samples of electrospun GelMA scaffolds were crosslinked in acetate frames (25 x 25 mm with an internal window of 15 x 15 mm; the frames were used to prevent shrinkage of the scaffold) as described above. Crosslinked scaffolds were cut away from the edges of the scaffold along the two sides parallel to the fibre direction using a scalpel. Scaffolds were then placed in a TA HDPlus Texture Analyser (Stable Micro Systems Ltd, Surrey, UK) with a 5-kg load cell with the fibre direction parallel to the testing direction. Samples were tested at an extension rate of 6 mm min^{-1}. Young's moduli of the samples were calculated from the resultant stress/strain curves.

2.8 Isolation and culture of primary rat aortic smooth muscle (AoSM) cells

Male Wistar rats (200-225g) were killed by stunning and exsanguination, using an approved Schedule 1 method of euthanasia. All procedures were approved by the animal welfare and ethical review body (AWERB) of the University of Nottingham. Rat aorta was dissected from the aortic arch to the abdominal aorta and placed in a zero Ca^{2+} dissection buffer solution (5.40 mM KCl, 137.0 mM NaCl, 0.50 mM $NaHPO_4$, 0.44 mM NaH_2PO_4, 10.0 mM glucose, 10.0 mM HEPES, 1.0 mM $MgCl_2$) on ice. The aorta was washed in ice-cold zero Ca^{2+} dissection buffer, excess connective tissue removed, then placed in a low Ca^{2+} dissection buffer (zero Ca^{2+} dissection buffer solution with the addition of 0.10 mM $CaCl_2$) and incubated at 37°C for

5 minutes. The aorta was cut into small sections and placed in 2 mL papain solution (≥15 units mL^{-1} papain from papaya latex, 5.83 mM 1,4-dithioerythritol, 0.90 mg mL^{-1} BSA)Sigma Aldrich) in low Ca2+ dissection buffer before incubation at 37°C for 45 minutes. The partially digested aortic tissue was extracted from the papain solution and washed in BSA solution (Sigma Aldrich) 3 times before transferring into 3 mL AoSMC media (high glucose DMEM supplemented with 10% (v/v) FBS and 1% (v/v) antibiotic/antimycotic solution (10000 units ml^{-1} penicillin G, 100 mg ml^{-1} streptomycin sulphate and 25 µg ml^{-1} amphotericin B). Tissue was firmly agitated by pipetting for 30 seconds to release cells from the partially digested tissue before the cell suspension was transferred into two collagen-coated (0.03 mg mL^{-1} type I bovine collagen (PureCol®, Advanced Biomatrix, San Diego, CA) in PBS) T-25 flasks containing 5 mL AoSMCs media. Flasks were incubated (at 37°C, 5% CO_2) for 48 hours before the media was changed to remove decellularised tissue and unattached cells; the cells were cultured for a further 5 days before the first passage. Subsequent passages were carried out every 7 days up to passage 3 in collagen-coated flasks; cells were used at passage 2-3.

2.9 PrestoBlue® cell viability assay

AoSMCs cell viability was measured post-seeding on aligned scaffolds using the PrestoBlue® assay at various time points across a 10-day period. Samples were washed with PBS prior to incubation with 1mL PrestoBlue working solution (10% (*v/v*) PrestoBlue in HASM culture media) for 10 minutes at 37 °C. PrestoBlue was then collected (100 µL aliquots) and replaced with media and the constructs returned to the incubator. Fluorescence was measured in duplicate on a Tecan Infinite M200 plate reader (Tecan, Reading, UK) using excitation and emission wavelengths of 560/590 nm. Resultant readings were expressed as a percentage of the fluorescence reading at day 0.

2.10 Immunocytochemistry

All samples were washed with PBS prior to fixation with 3.8% (*w/v*) *p*-formaldehyde for 10 minutes at room temperature. Samples were permeablised using 0.5% (*v/v*) Triton X-100 in PBS (5 minutes, 4°C) then blocked sequentially with 3% (*v/v*) BSA, 1% glycine (*w/v*) solution for one hour, followed by 10% (*v/v*) goat serum solution in PBS for 1 hour at room temperature. The following primary antibodies were used at 1:200 dilution in 10% (*v/v*) goat serum in PBS: α-smooth muscle actin (Alexa Fluor 488-conjugated phalloidin; Life Technologies, Paisley, UK), SM22α (ab14106; Abcam, Cambridge, MA), desmin (D1033; Sigma-Aldrich, UK),

connexin (C6219; Sigma-Aldrich, UK), vinculin (V4505; Sigma-Aldrich, UK) and calponin (ab46794; Abcam, Cambridge, MA). Samples were incubated with the relevant primary antibody at 4°C overnight. Nuclei were stained with Hoechst 33342 at a 1:833 dilution for 10 minutes (Fisher, UK). Samples were imaged using a Leica TCS SP2 laser scanning confocal inverted microscope (Leica Microsystems Ltd, Milton Keynes, UK) or a Leica DM2500 M fluorescent microscope. Images were then analysed using ImageJ. Nuclei alignment was calculated using particle analysis on binary images of Hoechst-stained cell nuclei. Surface coverage was determined by calculating the fraction of confocal *z*-stack images that were not stained for SM22α. SM marker positivity was calculated by counting the number of nuclei co-expressing the marker of interest and subtracting from the total nuclei present. Cell density was determined by dividing the number of nuclei visible per micrograph by micrograph area.

2.11 Scaffold contraction assays

Samples of crosslinked 10% *w/v* gelatin or GelMA scaffolds were placed in 6-well plates and sterilised by UV exposure (20 minutes), followed by incubation in media (60 minutes, 37°C) prior to cell seeding). Gelatin/GelMA scaffolds were seeded with AoSMCs at a density of 2x 10^5 cells cm^{-2} and incubated for 10 days at 37°C until confluency. Following incubation, culture media was aspirated and 1 mL serum-free DMEM added to each sample; scaffolds were cut out from their acetate frames and allowing them to be free-floating in the well-plates. Serum free DMEM (1 mL) ± smooth muscle contraction agonist, uridine 5'-triphosphate (200 μM UTP) was then added to each sample with minimum disturbance, allowed to equilibrate and imaged using a flatbed scanner at time intervals up to 30 minutes. Scanned images were analysed using ImageJ which was used to measure the surface area of the construct.

2.12 Direct force measurement of AoSMC-seeded GelMA scaffold contraction using muscle physiology apparatus

A force monitoring apparatus design has been previously reported by Dennis and Kosnik [30], and later adapted to measure the contractile force of cultured skeletal muscle constructs [31, 32]. This was further adapted here to measure uniaxial contractile force. Rectangular GelMA scaffolds (13x32 mm) were prepared, sterilised and seeded with AoSMCs at $2x10^5$ cells cm^{-2}. Scaffolds were then incubated for 10 days at 37°C until confluence when they were removed from culture media, washed twice with serum-free DMEM and individually placed in an 85-

mm petri dish containing a strip of canning wax adhered to the dish surface. Scaffolds were cut away from the acetate frames along the long axis of the scaffold (parallel to fibre direction) using a scalpel. One end of the scaffold was pinned in place by passing a minuten pin through the acetate frame into the canning wax. Serum-free DMEM (5 mL) was added to the dish and the acetate frame was cut away along the long axis to leave the scaffold free floating at one end. A minuten pin adhered to a glass bead was threaded through the underside of the scaffold at the free-floating end, which was then attached to a model 403A force transducer (Aurora Scientific, Dublin, Ireland) using canning wax **(Figure S2)**. The force transducer was connected to a Powerlab 4/25T unit with associated software (AD Instruments, Oxford, UK). Force was measured at a frequency of 1 kHz. Once stable, the baseline force of the resting scaffolds was measured for 3 minutes before the addition of 500 µL of 1 mM UTP in serum-free DMEM (500 µL serum free DMEM in control experiments) using a pipette (disturbance to the scaffolds was reduced to a minimum by careful pipetting). Contraction was then measured continuously for 60 minutes.

2.13 Statistical analysis

All statistical tests were carried out using the GraphPad Prism 6 (GraphPad Software Inc. San Diego, CA). Each statistical test carried out is stated in the relevant section and figure legends. Statistically significant results are represented with asterisk(s) (*, **, ***, ****) and represent p values ≤ 0.05, 0.01, 0.001 and 0.0001 respectively.

3. Results

The aim of this study was to develop a novel *in vitro* model of contractile smooth muscle tissue. We have previously shown that smooth muscle cells follow topographical cues from their environment; when cultured upon aligned electrospun PET scaffolds, the cells quickly formed an aligned population of cells [7, 33]. However, one noticeable feature of these scaffolds was that they were very stiff, with Young's moduli much higher than seen in *in vivo* muscle tissue [25]. To achieve a contractile SMC construct, we electrospun and crosslinked gelatin-based scaffolds that better mimic the mechanical properties of the extracellular matrix (ECM). These scaffolds were then seeded and cultured with rat aortic smooth muscle cells (AoSMCs), which were used as an exemplar smooth muscle cell type. The ability of these cells to align according to the aligned fibrous nature of the scaffolds, to express proteins associated with SMC

phenotype and the ability to measure contraction in response to chemical stimulus is presented here.

3.1 Electrospinning aligned gelatin fibre scaffolds

Gelatin was chosen due to its more elastic properties and its chemical similarity to collagen, which has been shown to allow the contraction of smooth muscle cells [34]. Gelatin was electrospun from solutions ranging 6% to 10% (*w/v*) (**Figure 1A**, **C** and **E**) to provide the topographical cues we had previously observed important for cell alignment [7, 33]. Scaffolds were crosslinked using EDC and NHS in an ethanol/water mixture with shrinkage prevented by securing the scaffolds in place during crosslinking using acetate frames (**Figure S1**). SEM images of the electrospun and crosslinked gelatin scaffolds are shown in **Figure 1B**, **D** and **F**.

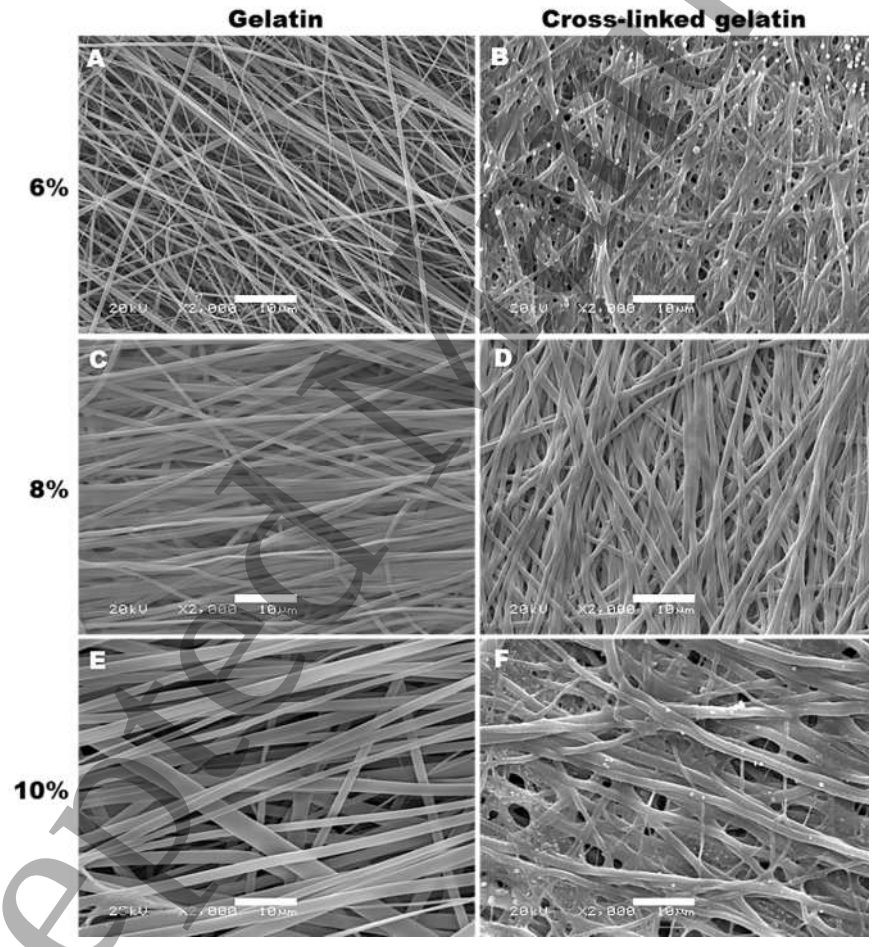

Figure 1: Electrospun gelatin scaffolds pre- and post-crosslinking. Representative SEM images of gelatin scaffolds electrospun from 6%, 8% and 10% w/v gelatin solutions (A,C,E respectively). The scaffolds were then imaged after cross-linking with ethyl-3-(3-dimethylaminopropyl) carbodiimide (EDC) and N-hydroxysuccinimide (NHS) (B,D,F). Scale bar = 10µm.

The average fibre diameter and degree of fibre alignment were analysed for each scaffold. Measurements were taken before and after the scaffolds were crosslinked to assess the effect of crosslinking on the morphology of the gelatin scaffolds. Fibre diameter of gelatin scaffolds increased with increasing concentration of the gelatin solution; 10% gelatin solutions produced fibres with an average diameter of 1.2 µm whereas 8% and 6% produced scaffolds with average fibre diameters of 788 and 286 nm respectively. Crosslinking of these scaffolds significantly affected the average fibre diameter with merging of individual fibres apparent (p<0.0001). In all cases, the average fibre diameter of the 10%, 8% and 6% gelatin scaffolds increased to 1.49 µm, 978 nm and 746 nm, an increase of 20%, 24% and 161% respectively (**Figure 2A**). All gelatin scaffolds were highly aligned, with 58%, 65% and 43% of fibres within 10° of the mean fibre angle in 10%, 8% and 6% scaffolds respectively which decreased in all cases (to 51%, 48% and 23% respectively) after the crosslinking process (**Figure 2B**).

Tensile testing was performed on crosslinked 6%, 8% and 10% (*w/v*) aligned gelatin scaffolds. Representative stress/strain curves for each scaffold are displayed in **Figure 2C**. The gradients of these curves were used to calculate the Young's modulus of each scaffold. The stiffest scaffold was that fabricated from 10% gelatin, with a mean Young's modulus value of 3.8 ± 1.7 MPa. The mean Young's moduli of the 8% and 6% gelatin scaffolds were 2.6 ± 0.7 and 1.5 ± 0.8 MPa respectively (mean ± SD). There was a statistical difference between the stiffness of the 10% and 6% gelatin scaffolds as shown in **Figure 2D** (p<0.05).

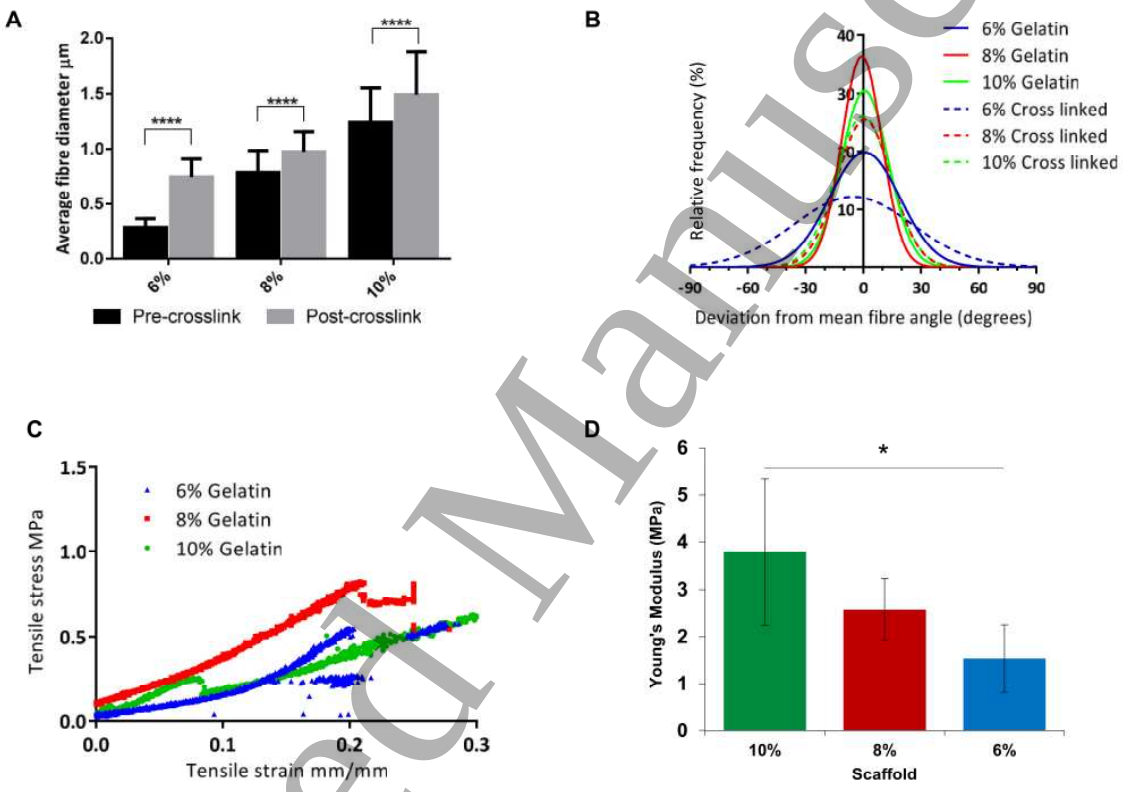

Figure 2: Properties of crosslinked electrospun gelatin scaffolds. (A) Average fibre diameters for each gelatin scaffold before and after crosslinking; error bars represent standard deviation (n=60, 20 measurements taken from 3 images of independent scaffolds). Unpaired *t*-tests were carried out between the fibre diameters of each scaffold before and after crosslinking. (B) Distribution curves illustrating the degree of alignment in each scaffold before and after crosslinking. (C) Representative stress/ strain curves for three different gelatin scaffolds. (D) Average Young's modulus for each scaffold (error bars represent standard deviation; *n*=6). One-way ANOVA with Tukey's multiple comparisons test was carried out between Young's moduli of all scaffolds ($p<0.05$).

3.2 Culture of AoSMCs on gelatin aligned fibre scaffolds

The differences seen in crosslinked gelatin scaffold alignment (10% > 8% > 6%) is reflected in the nuclear alignment of cells cultured upon the scaffolds. AoSMCs were more aligned when cultured on the 10% crosslinked gelatin scaffolds (38% within 10° of the mean) than on the 8% (27%) and 6% (21%) scaffolds (**Figure 3A**; a high magnification image illustrating nuclear alignment on the fibre scaffolds as identified by Hoescht staining is presented in **Figure 3F**). Due to the increased alignment of cells on 10% gelatin scaffolds, and demonstrating only a slight difference in stiffness compared to the other gelatin scaffolds, the 10% cross-linked gelatin scaffolds were chosen to be used for further cell culture studies.

Cell proliferation on the scaffolds was monitored using PrestoBlue (**Figure 3B**). Cellular metabolic activity increased steadily over the first 6 days of culture before a large increase between days 6 and 8. Confluency was achieved after 9 days when scaffolds were seeded at a density of 2 x 10^5 cells cm^{-2}. To confirm SM phenotype, cells cultured on the gelatin fibre scaffolds were immunostained and found to express the SM markers SM22α (**Figure 3C**) and calponin (**Figure 3E**). Cells also stained positive for the gap junction protein connexin, and negatively for the intermediate filament protein desmin (**Figure 3D**). Individual focal adhesions were observed in cells stained for vinculin (**Figure 3F**). Cells exhibited a spindle-like morphology, with most focal adhesions occurring at the spindle poles.

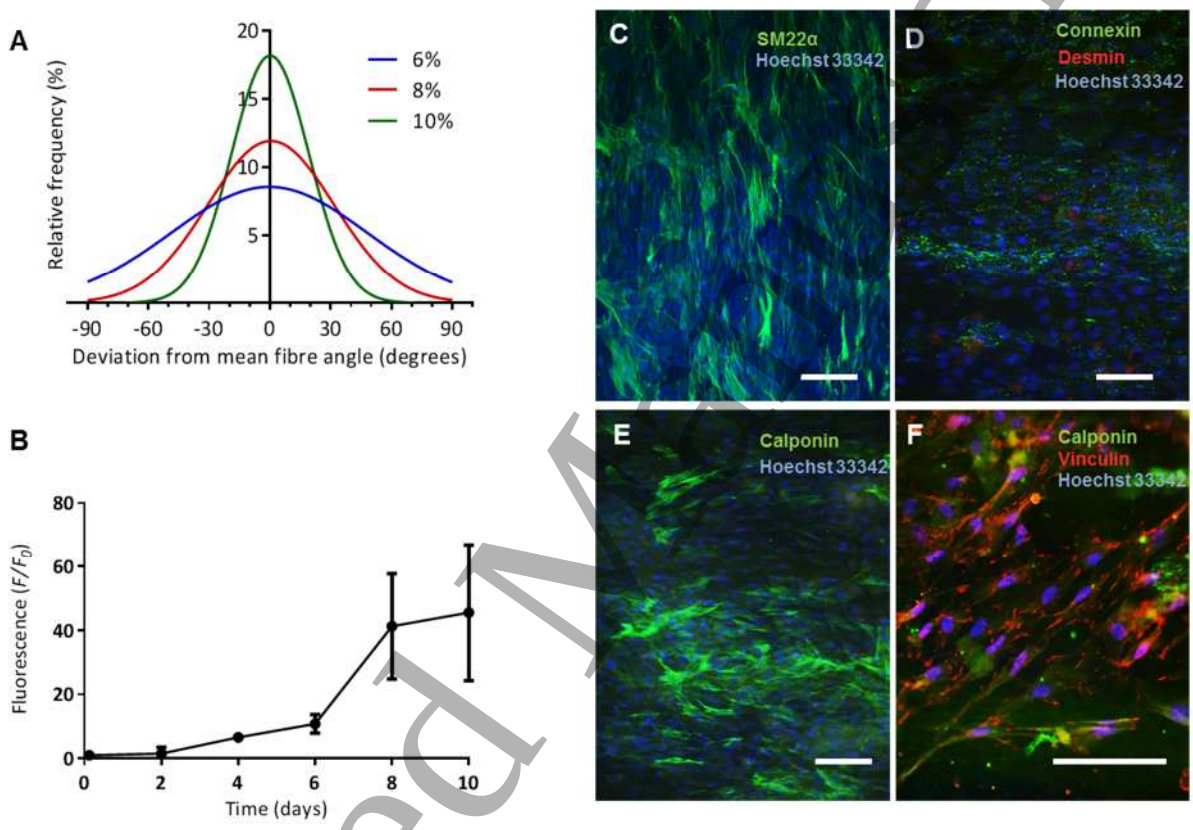

Figure 3: Culture of AoSMCs on crosslinked gelatin scaffolds. (A) Distribution curves illustrating the alignment of AoSMCs cultured on the cross-linked scaffolds. (B) Cell metabolism was monitored using the PrestoBlue® assay for 10 days. Error bars represent SEM; *n*=6. (C-F) AoSMCs were stained with SM22α (C), connexin (D) and calponin (E, F) (all green). Cells were also stained for desmin (D) and vinculin (F) (all red). All samples were additionally stained with Hoechst 33342 (blue). Scale bar = 100µm.

3.3 Contraction of AoSMCs seeded on gelatin (10%) fibre scaffolds

Crosslinked 10% gelatin electrospun scaffolds were seeded with AoSMCs at 2 x 10^5 cells cm^{-2} and incubated for 10 days before scaffolds were cut away from the supporting acetate frames. The cell-fibre constructs were submerged in media (free-floating) and the cells stimulated with 100 µM UTP and imaged to assess the degree of scaffold contraction. **Figure 4A** and **B** displays images of a cell-seeded gelatin scaffold at times *t*=0 and *t*=20 minutes respectively. By comparing the surface area of the construct across this period, constructs reduced to 90 ± 4.5% (mean ± SD) of their original size, and no further contraction was seen after 20 minutes (**Figure 4C and D**). Unstimulated controls remained approximately 100% their original size, with insignificant spontaneous contraction observed, throughout the study.

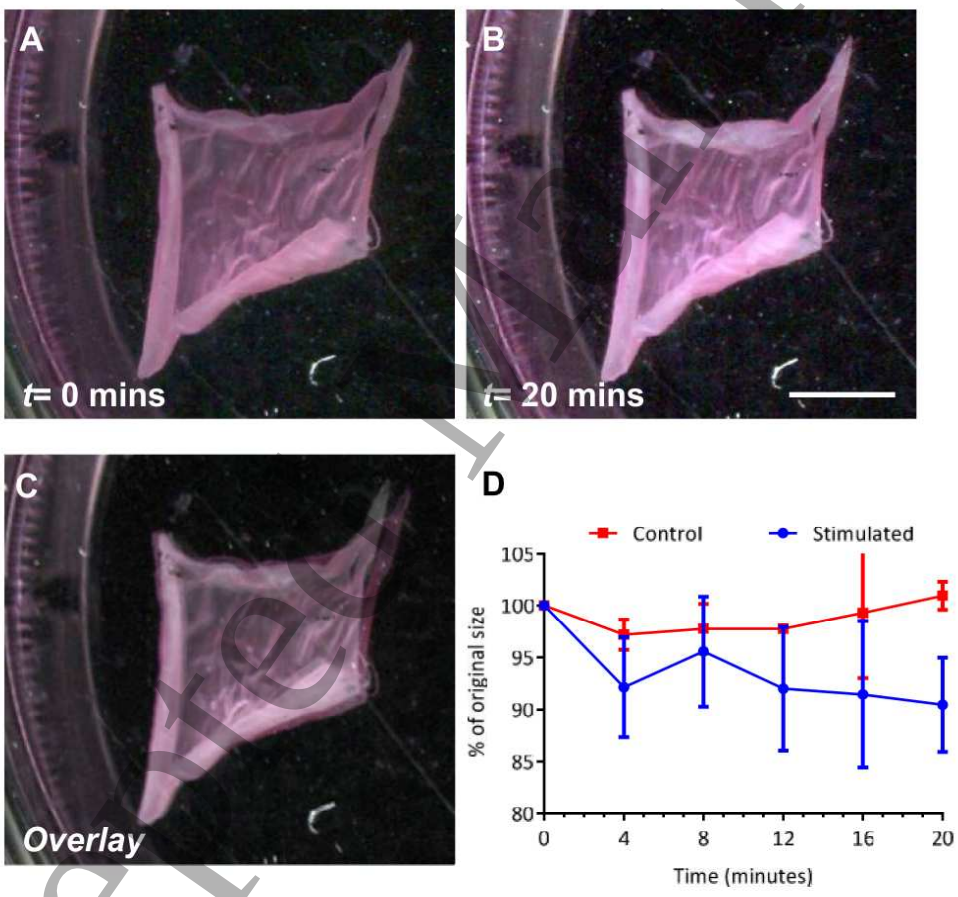

Figure 4: Contraction of AoSMC-seeded gelatin constructs. Scanned images of AoSMC-seeded gelatin scaffolds at *t*=0 (A) and *t*=20 minutes (B) following stimulation with UTP. Scale bar = 35 mm. To compare the constructs at the two time points, A has been overlaid onto image B, to give (C). Image analysis of the constructs at multiple time points was used to assess the level of construct contraction (D), error bars represent standard deviation (*n*=4).

3.4 Production of electrospun GelMA fibre scaffolds

Electrospinning of methacrylated gelatin (GelMA) was investigated provide a fibrous matrix with greater tenability to modulate the stiffness of the scaffold. The degree of gelatin methacrylation can be controlled by the ratio of gelatin:methacrylic anhydride in the initial reaction mixture in addition to length of exposure to UV light and concentration of photoinitiator. GelMA was synthesised in-house and the degree of methacrylation calculated using proton NMR spectroscopy (**Figure S4**). Comparing the ^{1}HNMR spectrum of synthesised GelMA to that of gelatin, there are two clear additional peaks in the GelMA spectrum at approximately 5.3 and 5.6 ppm due to the two protons found on the methacrylate vinyl group. The degree of methacrylation was calculated using a previously published method [18]. The peak at 0.84 ppm can be used as a reference peak ascribed to the hydrophobic side chains of valine, leucine and isoleucine; the integration of this peak ($I_{0.84}$) corresponds to 0.3836 mol/ 100 g (sum of known composition of these amino acids in gelatin). The total amount of available amine groups in gelatin is equal to 0.0385 mol/ 100g. Therefore, the percentage of methacrylation within the synthesised GelMA can be expressed using the following equation:

$$DM\% = I5.6ppm \times 0.3836 I0.84ppm \times 0.0385 \times 100$$

Using this equation, the percentage of methacrylation was calculated to be 81.0%.

The synthesised GelMA was electrospun using a 10% (*w/v*) solution as for the gelatin scaffolds (**Figure 5A**). SEM image analysis was used to determine the average fibre diameter (297.4 ± 101.1 nm (mean ± SD) and degree of fibre alignment (50% of fibres within 10° of the mean fibre angle) of the electrospun scaffolds. Distribution curves of the fibre diameter and angle are displayed in **Figure 5B** and **C** respectively. GelMA scaffolds were cut and adhered to acetate frames before being crosslinked using UV light in the presence of a photoinitiator (1% *w/v* solution of 2-Hydroxy-4′-(2-hydroxyethoxy)-2-methylpropiophenone). To prevent the GelMA scaffolds from dissolving during the crosslinking process, taking into account a single intensity UV lamp was used, a number of solvent mixtures were investigated. These ranged from pure ethanol to a 9:1 ethanol:water mixture. Scaffolds would not crosslink in pure ethanol and dissolved in solutions containing greater than 10% H_2O. Three different ethanol:water solutions were explored further including 39:1 (2.5% H_2O), 19:1 (5% H_2O) and 9:1 (10% H_2O). Tensile tests of the different crosslinked GelMA scaffolds showed that the Young's modulus increased with increasing water content in the crosslinking solution: average Young's moduli

were 142.2 ± 25.4, 158.7 ± 95.3 and 451.5 ± 111.3 kPa (mean ± SD) for scaffolds crosslinked in 2.5%, 5.0% and 10% water in ethanol solutions respectively (**Figure 5D**). Scaffolds crosslinked in 10% H_2O in ethanol were significantly stiffer than those crosslinked in 5% and 2.5% H_2O in ethanol solutions ($p<0.01$). Scaffold opacity increased with increasing crosslinking solution water content (**Figure 5E-G**). In addition, the failure rate of the scaffolds during post-crosslinking washing was much higher when crosslinking in 2.5% H_2O in ethanol. Individual fibre analysis post-crosslinking was not possible due to a lack of fibre resolution; fibres appeared to merge together during crosslinking although the aligned fibre morphology was evident when crosslinked in 5% and 10% H_2O in ethanol solutions (**Figure 5H,I**). Due to the high failure rates of 2.5% H_2O in ethanol-crosslinked scaffolds and the significantly higher Young's modulus of the 10% H_2O crosslinked scaffolds, scaffolds crosslinked in 5% H_2O in ethanol were chosen for the cell culture studies.

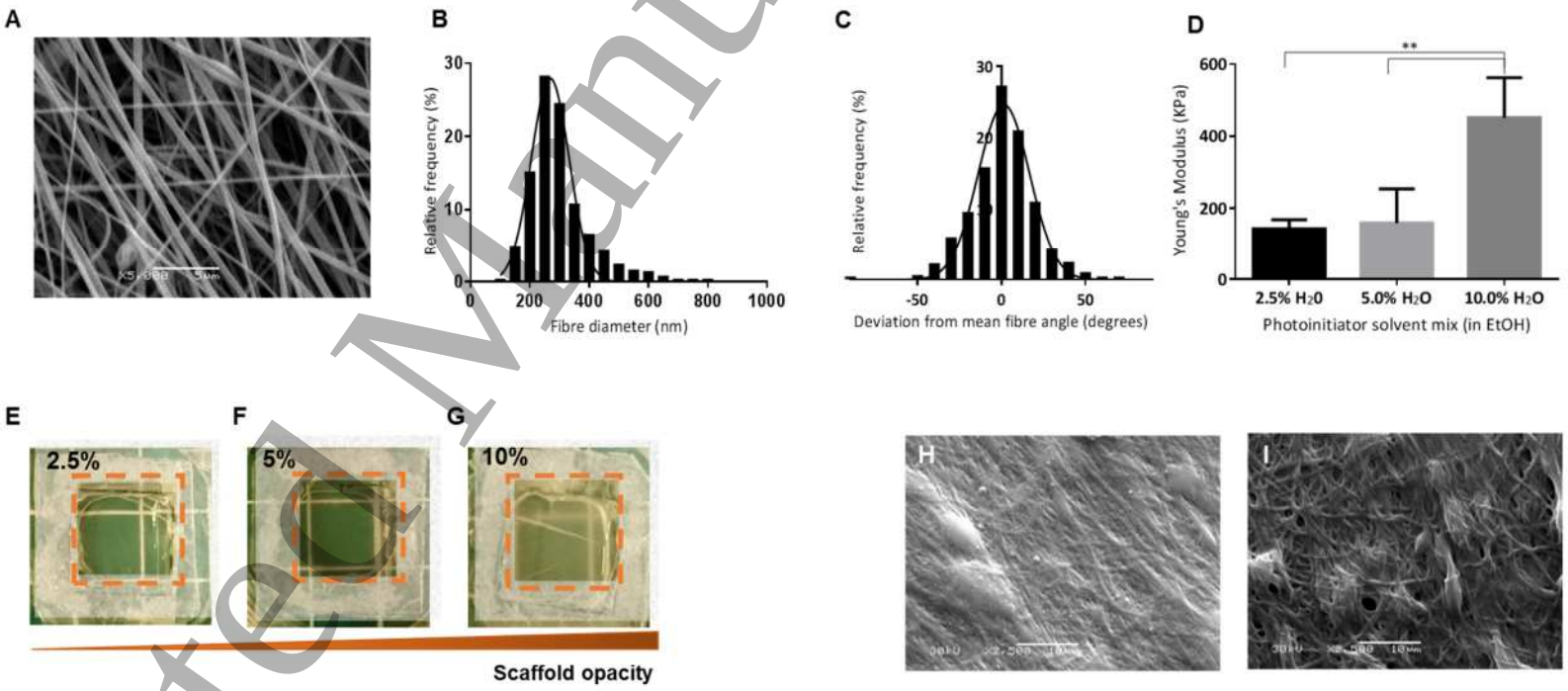

Figure 5: Properties of electrospun GelMA scaffolds. (A) SEM image of aligned electrospun GelMA spun from a 10% w/v solution before cross-linking. (B,C) Histograms and Gaussian distribution curves of fibre diameter (B) and fibre alignment (C) are presented (n=60, 20 measurements taken from 3 images of independent scaffolds). (D) Average Young's moduli of GelMA scaffolds crosslinked in different H_2O:EtOH mixtures. Error bars represent standard deviation (n=4). One way ANOVA with Tukey's multiple comparisons test was carried out between the Young's modulus of all scaffolds (p<0.01) (E, F, G). Representative photographs of scaffolds crosslinked in 2.5%, 5.0% and 10.0% (v/v) H2O in ethanol respectively, showing increasing scaffold opacity (scaffolds shown within dashed boxes). (H, I) SEM images of crosslinked GelMA scaffolds crosslinked in 5.0% (E) and 10.0% (F) H_2O.

3.5 Culture of AoSMCs on GelMA scaffolds

AoSMCs were cultured on crosslinked aligned GelMA scaffolds for a period of 10 days, during which cellular metabolic activity was monitored using the PrestoBlue® assay. Cell metabolism increased steadily throughout the 10-day period (**Figure 6A**), indicating cell proliferation over this time. Samples were fixed after 10 days and stained for the SM markers SM22α and calponin, and for the gap junction protein connexin (**Figure 6B, C** and **D** respectively). Samples stained positive for all markers and stained negatively for desmin (**Figure 6D**). Unlike AoSMCs cultured upon gelatin fibre scaffolds, those cultured upon GelMA fibre scaffolds did not stain positively for vinculin, with no clear focal adhesions present. Cell alignment on GelMA scaffolds was similar to the degree of alignment achieved on 8% and 6% gelatin scaffolds, with 23% of nuclei oriented within 10° of the mean (**Figure 6E**). A comparison of the morphological and mechanical properties of the scaffolds produced and smooth muscle ECM is shown in Table 1.

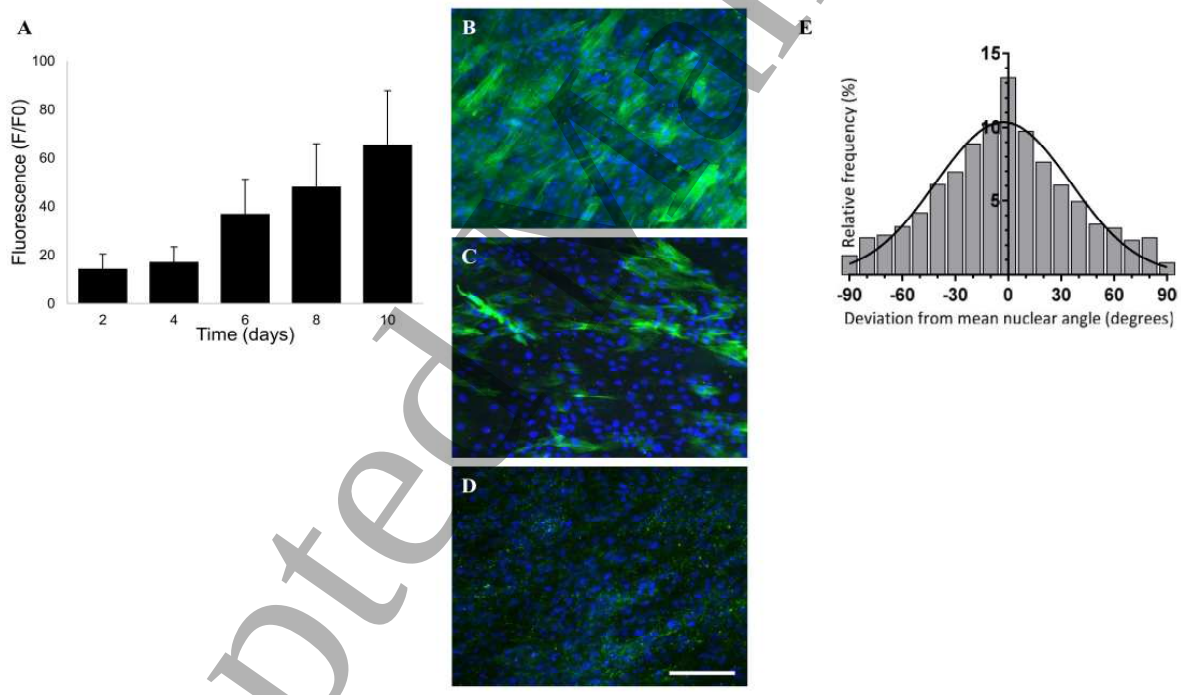

Figure 6: Culture of AoSMCs on crosslinked GelMA scaffolds. (A) AoSMCs were cultured on crosslinked GelMA scaffold for 10 days, cell metabolism was monitored periodically using the PrestoBlue® assay; error bars represent standard error of the mean (*n*=6). (B,C,D) Immunostaining of AoSMCs on electrospun GelMA scaffolds for SM22α (B), calponin (C), and connexin (D) (all green). Cells were also stained for desmin (D) and vinculin (C) (both red). All samples were additionally stained with Hoechst 33342 (blue). Scale bar = 100μm. (E) Samples

were fixed after 10 days and cell nuclei stained. Image analysis of stained samples was carried out in order to determine cell alignment (n=6).

Table 1: **Comparison of morphological and mechanical properties of the scaffolds produced in this study and smooth muscle ECM**

Material	*Gelatin Fibres*	*GelMA Fibres*	*Native SM ECM*
Average fibre diameter (µm)	1.24	0.38	--
Fibre alignment (% within 5° mean)	48	37	--
Nuclear Alignment (% within 10° mean)	38	23	65 [7]
Young's modulus (MPa)	1-4	0.15-0.45	0.15-0.9 [25]

3.6 Contraction of AoSMC-seeded GelMA fibre scaffolds

Crosslinked GelMA scaffolds were seeded with AoSMCs at a density of 2 x 10^5 cells cm^{-2} and incubated for 10 days before scaffolds were stimulated with 100 µM UTP and imaged to assess the degree of contraction. **Figures 7A and B** display images of a cell-seeded gelatin scaffold at times t=0 and t=30 minutes respectively. By comparing the construct's surface area across this period, AoSMCs contraction resulted in the reduction to 78 ± 2.5% (mean ± SD) of their original size (22% reduction in size), and no further contraction was observed after 30 minutes (**Figure 7C and D**). Unstimulated controls remained close to 100% their original size throughout the study. This level of contraction was higher than witnessed in the AoSMC-seeded gelatin scaffolds (reducing to 90 ± 4.5% of their original size). Following these results, the direct force measurement (using a force transducer) of AoSMC-seeded GelMA construct contraction was measured. AoSMCs were cultured upon crosslinked GelMA scaffolds for 10 days. After this culture period, constructs were cut from their acetate frames and attached to the force transducer (**Figure 7E**). Once attached, the force was allowed to stabilise before recording started. The stable force reading was measured for 3 minutes before the constructs were stimulated with 100 µM UTP. Control studies were stimulated with serum-free DMEM. An increase in force was detected within seconds of adding the agonist solution and continued to rise quickly for 20 minutes before slowing. Force measured continued to increase for a further 30 minutes before beginning to plateau (**Figure 7F**). The maximal force generated by the AoSMCs constructs ranged from 755.2 µN to 1356.4 µN, with the average max force being

1008.1 ± 251.6 µN (mean ± SD). The majority of contraction occurred within the first 5 minutes following stimulation, with 42 ± 3% of the maximal force measured occurring within this time; 60 ± 4% measured 10 minutes following stimulation and 95 ± 2% after 40 minutes stimulation.

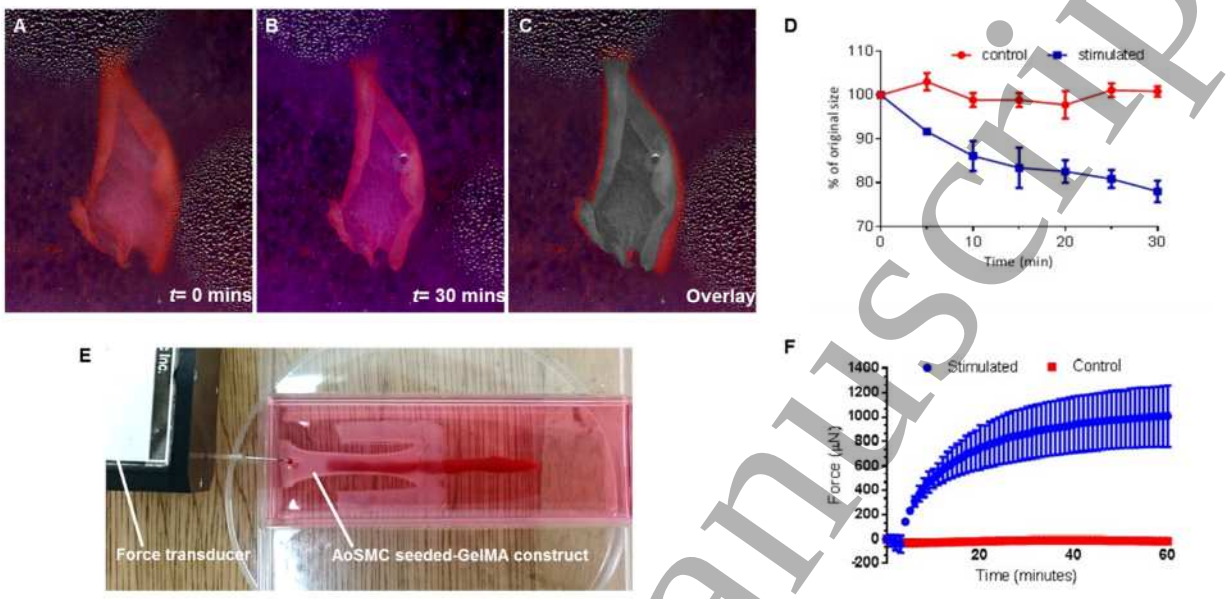

Figure 7: Contraction of AoSMC seeded GelMA scaffolds and direct force measurement of contraction of AoSMC seeded-GelMA constructs. (A-C) Scanned images of AoSMC-seeded GelMA construct at (A) *t*=0 and (B) *t*=30 minutes following stimulation with UTP. To compare the constructs at the two time points, A has been overlaid onto image B, to give C. (D) Image analysis of the constructs at multiple time points was used to assess the level of contraction, error bars represent standard deviation (*n*=3). (E) Photograph of AoSMC seeded-GelMA constructs contracting whilst attached to the force transducer. (F) Error bars represent standard deviation (*n*=4).

4 Discussion

The aim of this study was to develop an *in vitro* model of SM that possesses the ability to contract. This study explores the production of a range of electrospun crosslinked gelatin scaffolds which possess elastic properties and an aligned fibrous morphology to serve as a topographical cue to the cells. Primary rat aortic smooth muscle cells (AoSMCs) were explored as a model smooth muscle cell type, and the contraction of the cell-scaffold constructs in response to agonists were measured.

Given the wide range of polymers available when electrospinning, fibrous scaffolds can possess Young's moduli ranging from a few hundred kPa [35] to several hundred MPa [36].

This wide range in stiffness can greatly impact attachment [37], proliferation [38], and differentiation [39] of mammalian cells cultured upon them. It was therefore important to choose a material with mechanical properties that closely match the mechanical properties that cells experience *in vivo* to produce tissue constructs with functional outputs (such as contraction). In this study, the contractile behaviour of AoSMCs cultured upon electrospun scaffolds was explored. In addition, using the scaffold that supported SM contraction, the physical force generated during agonist-induced SM contraction was actively measured using muscle physiology apparatus.

In a previous study, HASM cells were cultured upon electrospun PET scaffolds for up to 14 days and expressed markers of a contractile SM phenotype [7]. In addition, we showed that HASM cells rapidly aligned on these scaffolds following the topographical cues from the fibres. However, the Young's modulus of *in vivo* SM is much lower than the Young's moduli of the PET scaffolds (200-300 MPa). For example, the Young's moduli of human arteries and porcine bronchi range from 0.1 to 1.0 MPa and 0.35 to 1.35 MPa respectively [25, 40]. These values are 100 to 1000 times lower than the values obtained for the PET scaffolds although some caution must be taken when comparing such values and native and synthetic materials are likely to have different porosities. As a result, a much less stiff material was required to provide suitable mechanical properties that would facilitate SM contraction. Gelatin was investigated, which is biocompatible, chemically similar to collagen, inexpensive, and possesses favourable mechanical properties.

Gelatin fibrous scaffolds were successfully fabricated using electrospinning. The fibre diameter increased with increasing gelatin concentration and ranged from 286 nm to 1.24 µm, a range similar to previously published work when similar concentrations of gelatin in fluorinated alcohols were electrospun [10, 38]. When gelatin is electrospun using aqueous solutions, much greater concentrations (30-40% *w/v*) need to be used to achieve similar sized fibres [12, 41]. This once again illustrates the effect that different electrospinning parameters (e.g.: solvent used) can have on the resultant fibres [42]. Scaffold fibre alignment was high for all scaffolds fabricated. Image analysis of the scaffolds after crosslinking showed that scaffolds appear slightly less uniform and the degree of alignment had decreased slightly. This is due to several fibres merging together during crosslinking as crosslinks formed between fibres, also leading to a reduction in visible pores between fibres; however, the aligned fibrous topography of the scaffolds remained. Crosslinking also resulted in an increase in fibre diameter in all of

the gelatin scaffolds; this has also been reported by Zhang *et al*. [12], who crosslinked gelatin scaffolds with EDC and NHS at 25mM EDC. Fibre swelling, due to absorption of water, has also been reported when crosslinking gelatin scaffolds with genipin [41]. In this case, the crosslinked scaffolds appear to behave like a hydrogel, swelling in size with reduced stiffness, whilst retaining their fibrous structure. Zhang *et al*. also found that when wet, the Young's modulus of crosslinked gelatin scaffolds dramatically decreases [12]. As the scaffolds produced in this study were to be used for cell culture, only the wet state Young's modulus was measured, which ranged from 3.80 to 1.54 MPa – values similar in magnitude to those measured by Zhang for similar sized scaffolds. Future work will determine the mechanical properties of individual fibres using atomic force microscopy to identify the forces experienced by individual cells [50].

Scaffolds spun from 10% *w/v* gelatin solutions were chosen to assess cell attachment, proliferation and phenotype. AoSMCs displayed high alignment when cultured upon the scaffolds. Cells achieved confluency over 9 days with increasing metabolic activity over the same period, signifying that cells were proliferating on the scaffolds. Immunostaining for SM22α and calponin showed that both proteins were present, in addition to illustrating the aligned, spindle-shaped morphology of the cells, all of which are indicative of a contractile SM phenotype. In addition, cells stained positive for the gap junction protein connexin, with gap junctions visible between cells. Focal adhesions were also seen on scaffolds, with cells staining positive for vinculin. Once again, cells stained negative for desmin. Vascular smooth muscle cells possess little to no desmin, with vimentin being the key constituent of intermediate filaments [43].

Few studies have investigated the contractile force generated by seeding SM cells onto materials [2, 44, 45]. Very few have directly measured this force, and those that did were carried out on cell-seeded collagen hydrogels [46]. In this study, cell-seeded constructs were stimulated with 100 μM UTP and imaged periodically to measure scaffold contraction. Scaffolds reduced in size by an average of 9.5% over 20 minutes following stimulation relative to unstimulated controls. Although the level of contraction was small, it was deemed possible to create AoSMC-seeded electrospun aligned scaffold constructs that contract by reducing scaffold stiffness further.

Due to the multiple ways in which the mechanical properties of GelMA hydrogels can be manipulated, GelMA was considered as an attractive material that could potentially produce

electrospun scaffolds with Young's moduli lower than those seen in the gelatin scaffolds by varying the degree of cross-linking. GelMA was successfully synthesised following a previously published method [14, 17]. The level of GelMA crosslinking can be controlled by the initial level of methacrylation, the amount of photoinitiator used, the length of UV exposure and the solvents used in the crosslinking process. Following synthesis, the degree of methacrylation of gelatin was calculated using NMR spectra and found to be approximately 80%. This level of methacrylation matches previously published calculated values for the same gelatin: methacrylic anhydride ratio (degree of methacrylation of ~70 - 80%) [14, 17].

Synthesised GelMA was electrospun at a concentration of 10% *w/v* generating aligned fibres around 300 nm in diameter, which were much thinner compared to gelatin fibres electrospun from the equivalent concentration (average diameter of 1.2 μm). This is most probably due to a change in the overall net charge of the molecule during GelMA synthesis, whereby consumption of the majority of free amines by methacrylation (and no change to the number of free carboxylate groups) led to an increased negative charge at neutral pH due to the presence of deprotonated carboxylic acid groups [47]. This in turn affected the conductivity of the electrospinning solution, leading to thinner fibres. A crosslinking method had to be developed where the scaffolds retained their fibrous architecture whilst submerged in a photoinitiator solution. Previous studies have crosslinked GelMA hydrogels in PBS [14, 17, 18], but this was not possible with the electrospun scaffolds due to the high solubility of these GelMA fibres upon contact with aqueous solutions. In order to overcome this issue, the EDC and NHS gelatin crosslinking method was adapted [12], which utilises a 9:1 ethanol:water mix for crosslinking. A range of ethanol:water mixtures were investigated for use as the solvent for the photoinitiator solution. Mixtures with a water content higher than 10% (*v/v*) caused the scaffolds to dissolve, and those with a water content of less than 2.5% failed to sufficiently crosslink scaffolds under UV light, leading to dissolution of the scaffolds upon washing with PBS. By changing the ethanol to water ratio it was possible to partially control the level of GelMA crosslinking and, as a result, the mechanical properties of the scaffolds. Young's moduli of the scaffolds ranged from 142 kPa (2.5% water) to 451 kPa (10% water) which was in line with values published for human arteries (0.1 to 1.0 MPa [25]). SEM images of crosslinked scaffolds suggested that scaffolds appeared to lose their porous structure due to fibre swelling upon crosslinking, but the aligned fibrous topography of scaffolds was still visible.

AoSMCs were cultured upon GelMA scaffolds crosslinked in a 5% water in ethanol solution. These scaffolds were chosen for further cell culture experiments due to their low Young's modulus and high crosslinking success rate relative to 10% and 2.5% (crosslinking solution water in ethanol) respectively. As with gelatin scaffolds, cells proliferated on the surface of the GelMA scaffolds over a 10 day period and aligned upon the scaffolds, indicating that the surface topography of the scaffolds remained sufficiently intact after crosslinking to provide mechanical cues to the cells. The degree of nuclear alignment was lower when cells were cultured on the GelMA scaffolds than on the PET scaffolds (23 vs 49% of cells within 10° of the mean; [7]), which correlates with the loss of alignment seen when crosslinking the GelMA scaffolds. AoSMCs once again stained positive for SM22α, calponin and connexion. Unlike when cultured on gelatin scaffolds, AoSMCs on GelMA scaffolds showed no clear positive staining for vinculin, signifying that no focal adhesion points could be identified. It has been previously documented that the level of vinculin bound to the cytoskeleton, and the amount of vinculin localizing at focal adhesions is larger on stiffer surfaces than on more elastic ones [48, 49]. The difference in stiffness between the GelMA and gelatin scaffolds could therefore be the reason why no vinculin localisation was seen on the GelMA scaffolds. As previously attempted with the gelatin scaffolds, AoSMCs were cultured upon square crosslinked electrospun GelMA scaffolds for 10 days prior to contraction studies. When stimulated to contract with 100 µM UTP, the AoSMC-seeded GelMA constructs reduced in surface area by an average of 22% due to AoSMCs contraction. Since this level of contraction was higher than that seen in AoSMC-seeded gelatin constructs, GelMA scaffolds were chosen to be used for the measurement of the physical force exerted by SM cells during contraction.

AoSMCs were seeded on crosslinked GelMA scaffolds and cultured for 10 days to achieve a confluent layer of cells. These constructs were then attached to the force transducer and stimulated with 100 µM UTP; these constructs contracted instantly and generated average maximal forces in the region of 1000 µN. Although electrospun gelatin scaffolds have been used to produce contractile tissues such as cardiac [35] and skeletal [50] muscle previously, this is the first time that SM contraction has been assessed using electrospun scaffolds. In addition, this is also the first time that the physical force of contraction from any cell type has been directly measured on electrospun scaffolds. In addition, the ability to modulate the stiffness of the scaffold allows the impact of matrix stiffness, relevant in the study of

inflammatory diseases such as asthma where tissue remodelling occurs, upon cell phenotype and function to be studied

5 Conclusions

This work represents the first time that the contractile forces generated by a confluent, aligned sheet of SM cells cultured upon gelatin based electrospun scaffolds have been directly measured. We also describe novel methods for the crosslinking of electrospun GelMA scaffolds. Using these methods, the mechanical properties of the GelMA scaffolds were manipulated by controlling the amount of water in the ethanol based photoinitiator solution. SM cells readily attached to, proliferated and aligned upon both gelatin and GelMA fibrous scaffolds, expressing contractile SM markers in all cases. SM cells were able to contract both gelatin and GelMA scaffolds, with greater contraction seen on the less stiff GelMA scaffolds. This *in vitro* model of contractile smooth muscle holds great potential for the study of disease arising from matrix remodelling and in the discovery of new therapeutic entities to treat such diseases.

6 Acknowledgements

This work was funded by the Engineering and Physical Research Centre (EPSRC) Doctoral Training Centre (DTC; EP/F500491/1; studentship awarded to JC Bridge) in Regenerative Medicine, U.K. GE Morris was employed on a related project funded by the National Centre for the Replacement, Refinement, and Reduction of Animals in Research (NC3Rs; G1001804/1). We also wish to acknowledge Dr William Dunn at the University of Nottingham for the procurement of rat aortas for the isolation of aortic smooth muscle cells.

7 References

[1] S.T. Holgate, H.S. Arshad, G.C. Roberts, P.H. Howarth, P. Thurner, D.E. Davies, A new look at the pathogenesis of asthma, Clin Sci 118(7-8) (2010) 439-450.

[2] A.R. West, N. Zaman, D.J. Cole, M.J. Walker, W.R. Legant, T. Boudou, C.S. Chen, J.T. Favreau, G.R. Gaudette, E.A. Cowley, G.N. Maksym, Development and characterization of a 3D multicell microtissue culture model of airway smooth muscle, Am J Physiol Lung Cell Mol Physiol 304(1) (2013) L4-16.

[3] J.H. Bates, M. Rincon, C.G. Irvin, Animal models of asthma, Am J Physiol Lung Cell Mol Physiol 297(3) (2009) L401-10.

[4] L.G. Griffith, M.A. Swartz, Capturing complex 3D tissue physiology in vitro, Nat Rev Mol Cell Biol 7(3) (2006) 211-24.

[5] H.M. Powell, D.M. Supp, S.T. Boyce, Influence of electrospun collagen on wound contraction of engineered skin substitutes, Biomaterials 29(7) (2008) 834-843.

[6] S. Hinds, W. Bian, R.G. Dennis, N. Bursac, The role of extracellular matrix composition in structure and function of bioengineered skeletal muscle, Biomaterials 32(14) (2011) 3575-83.

[7] G.E. Morris, J.C. Bridge, O.M.I. Eltboli, A.J. Knox, J.W. Aylott, C.E. Brightling, A.M. Ghaemmaghami, F.R.A.J. Rose, Human airway smooth muscle maintain in situ cell orientation and phenotype when cultured on aligned electrospun scaffolds, Am J Physiol-Lung C 307(1) (2014) L38-L47.

[8] T. Liu, W.K. Teng, B.P. Chan, S.Y. Chew, Photochemical crosslinked electrospun collagen nanofibers: Synthesis, characterization and neural stem cell interactions, J Biomed Mater Res A 95a(1) (2010) 276-282.

[9] L. Yang, C.F.C. Fitie, K.O. van der Werf, M.L. Bennink, P.J. Dijkstra, J. Feijen, Mechanical properties of single electrospun collagen type I fibers, Biomaterials 29(8) (2008) 955-962.

[10] S.W. Tsai, H.M. Liou, C.J. Lin, K.L. Kuo, S. Hung, R.C. Weng, F.Y. Hsu, MG63 Osteoblast-Like Cells Exhibit Different Behavior when Grown on Electrospun Collagen Matrix versus Electrospun Gelatin Matrix, Plos One 7(2) (2012).

[11] M.K. Yeh, Y.M. Liang, K.M. Cheng, N.T. Dai, C.C. Liu, J.J. Young, A novel cell support membrane for skin tissue engineering: Gelatin film cross-linked with 2-chloro-1-methylpyridinium iodide, Polymer 52(4) (2011) 996-1003.

[12] S. Zhang, Y. Huang, X. Yang, F. Mei, Q. Ma, G. Chen, S. Ryu, X. Deng, Gelatin nanofibrous membrane fabricated by electrospinning of aqueous gelatin solution for guided tissue regeneration, J Biomed Mater Res A 90(3) (2009) 671-9.

[13] A.I. Van den Bulcke, B. Bogdanov, N. De Rooze, E.H. Schacht, M. Cornelissen, H. Berghmans, Structural and rheological properties of methacrylamide modified gelatin hydrogels, Biomacromolecules 1(1) (2000) 31-38.

[14] J.W. Nichol, S.T. Koshy, H. Bae, C.M. Hwang, S. Yamanlar, A. Khademhosseini, Cell-laden microengineered gelatin methacrylate hydrogels, Biomaterials 31(21) (2010) 5536-44.

[15] Y. Zuo, X. Liu, D. Wei, J. Sun, W. Xiao, H. Zhao, L. Guo, Q. Wei, H. Fan, X. Zhang, Photo-cross-linkable methacrylated gelatin and hydroxyapatite hybrid hydrogel for modularly engineering biomimetic osteon, ACS Appl Mater Interfaces 7(19) (2015) 10386-94.

[16] X. Zhao, Q. Lang, L. Yildirimer, Z.Y. Lin, W. Cui, N. Annabi, K.W. Ng, M.R. Dokmeci, A.M. Ghaemmaghami, A. Khademhosseini, Photocrosslinkable Gelatin Hydrogel for Epidermal Tissue Engineering, Adv Healthc Mater 5(1) (2016) 108-18.

[17] M. Nikkhah, N. Eshak, P. Zorlutuna, N. Annabi, M. Castello, K. Kim, A. Dolatshahi-Pirouz, F. Edalat, H. Bae, Y. Yang, A. Khademhosseini, Directed endothelial cell morphogenesis in micropatterned gelatin methacrylate hydrogels, Biomaterials 33(35) (2012) 9009-18.

[18] A. Ovsianikov, A. Deiwick, S. Van Vlierberghe, P. Dubruel, L. Moller, G. Drager, B. Chichkov, Laser fabrication of three-dimensional CAD scaffolds from photosensitive gelatin for applications in tissue engineering, Biomacromolecules 12(4) (2011) 851-8.

[19] L.E. Bertassoni, J.C. Cardoso, V. Manoharan, A.L. Cristino, N.S. Bhise, W.A. Araujo, P. Zorlutuna, N.E. Vrana, A.M. Ghaemmaghami, M.R. Dokmeci, A. Khademhosseini, Direct-write bioprinting of cell-laden methacrylated gelatin hydrogels, Biofabrication 6(2) (2014) 024105.

[20] K. Yue, G. Trujillo-de Santiago, M.M. Alvarez, A. Tamayol, N. Annabi, A. Khademhosseini, Synthesis, properties, and biomedical applications of gelatin methacryloyl (GelMA) hydrogels, Biomaterials 73 (2015) 254-71.

[21] Y. Liu, M.B. Chan-Park, A biomimetic hydrogel based on methacrylated dextran-graft-lysine and gelatin for 3D smooth muscle cell culture, Biomaterials 31(6) (2010) 1158-70.

[22] T.R. Correia, P. Ferreira, R. Vaz, P. Alves, M.M. Figueiredo, I.J. Correia, P. Coimbra, Development of UV cross-linked gelatin coated electrospun poly(caprolactone) fibrous scaffolds for tissue engineering, Int J Biol Macromol 93(Pt B) (2016) 1539-1548.

[23] X.M. Sun, Q. Lang, H.B. Zhang, L.Y. Cheng, Y. Zhang, G.Q. Pan, X. Zhao, H.L. Yang, Y.G. Zhang, H.A. Santos, W.G. Cui, Electrospun Photocrosslinkable Hydrogel Fibrous Scaffolds for Rapid In Vivo Vascularized Skin Flap Regeneration, Adv Funct Mater 27(2) (2017).

[24] X. Zhao, X. Sun, L. Yildirimer, Q. Lang, Z.Y. Lin, R. Zheng, Y. Zhang, W. Cui, N. Annabi, A. Khademhosseini, Cell infiltrative hydrogel fibrous scaffolds for accelerated wound healing, Acta Biomater 49 (2017) 66-77.

[25] W.A. Riley, R.W. Barnes, G.W. Evans, G.L. Burke, Ultrasonic measurement of the elastic modulus of the common carotid artery. The Atherosclerosis Risk in Communities (ARIC) Study, Stroke 23(7) (1992) 952-6.

[26] A.M. Holmes, R. Solari, S.T. Holgate, Animal models of asthma: value, limitations and opportunities for alternative approaches, Drug Discov Today 16(15-16) (2011) 659-70.

[27] C.E. Schmidt, J.M. Baier, Acellular vascular tissues: natural biomaterials for tissue repair and tissue engineering, Biomaterials 21(22) (2000) 2215-31.

[28] S.K. Yazdani, B. Watts, M. Machingal, Y.P. Jarajapu, M.E. Van Dyke, G.J. Christ, Smooth muscle cell seeding of decellularized scaffolds: the importance of bioreactor preconditioning to development of a more native architecture for tissue-engineered blood vessels, Tissue Eng Part A 15(4) (2009) 827-40.

[29] A.J. Kuijpers, G.H. Engbers, J. Krijgsveld, S.A. Zaat, J. Dankert, J. Feijen, Cross-linking and characterisation of gelatin matrices for biomedical applications, J Biomater Sci Polym Ed 11(3) (2000) 225-43.

[30] R.G. Dennis, P.E. Kosnik, 2nd, Excitability and isometric contractile properties of mammalian skeletal muscle constructs engineered in vitro, In Vitro Cell Dev Biol Anim 36(5) (2000) 327-35.

[31] Y.C. Huang, R.G. Dennis, L. Larkin, K. Baar, Rapid formation of functional muscle in vitro using fibrin gels, J Appl Physiol 98(2) (2005) 706-713.

[32] A. Khodabukus, K. Baar, Regulating Fibrinolysis to Engineer Skeletal Muscle from the C2C12 Cell Line, Tissue Eng Part C-Me 15(3) (2009) 501-511.

[33] J.C. Bridge, J.W. Aylott, C.E. Brightling, A.M. Ghaemmaghami, A.J. Knox, M.P. Lewis, F.R. Rose, G.E. Morris, Adapting the Electrospinning Process to Provide Three Unique Environments for a Tri-layered In Vitro Model of the Airway Wall, J Vis Exp (101) (2015) e52986.

[34] H. Matsumoto, L.M. Moir, B.G. Oliver, J.K. Burgess, M. Roth, J.L. Black, B.E. McParland, Comparison of gel contraction mediated by airway smooth muscle cells from patients with and without asthma, Thorax 62(10) (2007) 848-54.

[35] M. Kharaziha, M. Nikkhah, S.R. Shin, N. Annabi, N. Masoumi, A.K. Gaharwar, G. Camci-Unal, A. Khademhosseini, PGS:Gelatin nanofibrous scaffolds with tunable mechanical and structural properties for engineering cardiac tissues, Biomaterials 34(27) (2013) 6355-66.

[36] A. Hadjizadeh, A. Ajji, M.N. Bureau, Nano/micro electro-spun polyethylene terephthalate fibrous mat preparation and characterization, J Mech Behav Biomed Mater 4(3) (2011) 340-51.

[37] M.G. Haugh, C.M. Murphy, R.C. McKiernan, C. Altenbuchner, F.J. O'Brien, Crosslinking and mechanical properties significantly influence cell attachment, proliferation, and migration within collagen glycosaminoglycan scaffolds, Tissue Eng Part A 17(9-10) (2011) 1201-8.

[38] M. Skotak, S. Noriega, G. Larsen, A. Subramanian, Electrospun cross-linked gelatin fibers with controlled diameter: the effect of matrix stiffness on proliferative and biosynthetic activity of chondrocytes cultured in vitro, J Biomed Mater Res A 95(3) (2010) 828-36.

[39] J.S. Park, J.S. Chu, A.D. Tsou, R. Diop, Z.Y. Tang, A.J. Wang, S. Li, The effect of matrix stiffness on the differentiation of mesenchymal stem cells in response to TGF-beta, Biomaterials 32(16) (2011) 3921-3930.

[40] J.-Y. Wang, P. Mesquida, P. Pallai, C.J. Corrigan, T.H. Lee, Dynamic Properties of Human Bronchial Airway Tissues, eprint arXiv:1111.5645 (2011).

[41] S. Panzavolta, M. Gioffre, M.L. Focarete, C. Gualandi, L. Foroni, A. Bigi, Electrospun gelatin nanofibers: Optimization of genipin cross-linking to preserve fiber morphology after exposure to water, Acta Biomaterialia 7(4) (2011) 1702-1709.

[42] F.A.A. Ruiter, C. Alexander, F.R.A.J. Rose, J.I. Segal, A design of experiments approach to identify the influencing parameters that determine poly-D, L-lactic acid (PDLLA) electrospun scaffold morphologies, Biomed Mater 12(5) (2017).

[43] G. Gabbiani, E. Schmid, S. Winter, C. Chaponnier, C. de Ckhastonay, J. Vandekerckhove, K. Weber, W.W. Franke, Vascular smooth muscle cells differ from other smooth muscle cells: predominance of vimentin filaments and a specific alpha-type actin, Proc Natl Acad Sci U S A 78(1) (1981) 298-302.

[44] A. Grosberg, A.P. Nesmith, J.A. Goss, M.D. Brigham, M.L. McCain, K.K. Parker, Muscle on a chip: in vitro contractility assays for smooth and striated muscle, J Pharmacol Toxicol Methods 65(3) (2012) 126-35.

[45] A.P. Nesmith, A. Agarwal, M.L. McCain, K.K. Parker, Human airway musculature on a chip: an in vitro model of allergic asthmatic bronchoconstriction and bronchodilation, Lab Chip 14(20) (2014) 3925-36.

[46] K. Oishi, Y. Itoh, Y. Isshiki, C. Kai, Y. Takeda, K. Yamaura, H. Takano-Ohmuro, M.K. Uchida, Agonist-induced isometric contraction of smooth muscle cell-populated collagen gel fiber, Am J Physiol Cell Physiol 279(5) (2000) C1432-42.

[47] L. Zhou, G.X. Tan, Y. Tan, H. Wang, J.W. Liao, C.Y. Ning, Biomimetic mineralization of anionic gelatin hydrogels: effect of degree of methacrylation, Rsc Adv 4(42) (2014) 21997-22008.

[48] H. Yamashita, T. Ichikawa, D. Matsuyama, Y. Kimura, K. Ueda, S.W. Craig, I. Harada, N. Kioka, The role of the interaction of the vinculin proline-rich linker region with vinexin alpha in sensing the stiffness of the extracellular matrix, J Cell Sci 127(Pt 9) (2014) 1875-86.

[49] D.E. Discher, P. Janmey, Y.L. Wang, Tissue cells feel and respond to the stiffness of their substrate, Science 310(5751) (2005) 1139-43.

[50] S. Ostrovidov, X. Shi, L. Zhang, X. Liang, S.B. Kim, T. Fujie, M. Ramalingam, M. Chen, K. Nakajima, F. Al-Hazmi, H. Bae, A. Memic, A. Khademhosseini, Myotube formation on gelatin nanofibers - multi-walled carbon nanotubes hybrid scaffolds, Biomaterials 35(24) (2014) 6268-77.

[51] P. Dutov, O Antipova, S Varma, JPRO Orgel, JD Schieber. Measurement of Elastic Modulus of Collagen Type I Single Fiber. PLoS ONE 11(1) (2016) e0145711.